

## Possible Linkage between the Monsoon Trough Variability and the Tropical Cyclone Activity over the Western North Pacific

LIANG WU

*Center for Monsoon System Research, Institute of Atmospheric Physics, Chinese Academy of Sciences, Beijing, and Center for Monsoon and Environment Research/Department of Atmospheric Sciences, Sun Yat-sen University, Guangzhou, China*

ZHIPING WEN

*Center for Monsoon and Environment Research/Department of Atmospheric Sciences, Sun Yat-sen University, Guangzhou, China*

RONGHUI HUANG

*Center for Monsoon System Research, Institute of Atmospheric Physics, Chinese Academy of Sciences, Beijing, China*

RENGUANG WU

*Institute of Space and Earth Information Science, and Department of Physics, The Chinese University of Hong Kong, Hong Kong, China*

(Manuscript received 22 March 2011, in final form 19 June 2011)

### ABSTRACT

The present study investigates the influence of the monsoon trough (MT) on the interannual variability of tropical cyclone (TC) activity over the western North Pacific during July–November for the period 1979–2007. It is shown that the TC activity is closely related to the MT location. During the years when the MT extends eastward (retreats westward), more (less) TCs form within the southeastern quadrant of the western North Pacific. Such a relationship can be explained by the changes in large-scale environmental factors associated with the movement of the MT. An eastward extension of the MT coincides with warmed ocean surface, enhanced convection, increased relative humidity in the lower and midtroposphere, reduced vertical shear of zonal wind, intensified upper-level divergence, and low-level anomalous cyclonic vorticity over the southeast quadrant of the western North Pacific. These conditions associated with the eastern extension of the MT are favorable for TC genesis, while those associated with the westward retreat of the MT are not. Diagnosis of the barotropic energy conversion indicates that synoptic-scale disturbances moving westward from tropical eastern Pacific will gain the energy from the mean flow when they meet with the eastward-extending MT. This is an important reason for the linkage between MT variability and TC genesis over the western North Pacific.

### 1. Introduction

It has long been recognized that tropical cyclone (TC) activity over the western North Pacific (WNP) has a distinct signal of interannual variations (Landsea 2000). Previous studies have shown that a longitudinal shift in the location of TC formation occurs in El Niño–Southern

Oscillation (ENSO) years (e.g., Camargo and Sobel 2005; Camargo et al. 2007; Chan 1985, 2000; Wang and Chan 2002). The interannual variations of the WNP TC activity are closely related to several changes in atmospheric thermodynamics and dynamics. In summer and fall, the large-scale low-level circulation over the WNP features low-latitude southwesterlies, a monsoon trough (MT), and a subtropical ridge (Lander 1996). The WNP MT is the near-equatorial confluence zone between the low-level easterly trade winds and the westerly monsoonal wind (Briegel 2002; Chan and Evans 2002; Tomita et al. 2004). It is often associated with deep convection that

---

*Corresponding author address:* Prof. Zhiping Wen, Center for Monsoon and Environment Research/Department of Atmospheric Sciences, Sun Yat-sen University, Guangzhou 510275, China.  
E-mail: eeswzp@mail.sysu.edu.cn

enhances the cyclonic flow by diabatic heating (Holland 1995; Webster 1980). Climatologically, the MT over the WNP extends along the southwestern periphery of the subtropical high. The evolution of the MT is closely related to the movement of the WNP subtropical high (Lau and Li 1984; Wang and Wu 1997). An eastward retreat of the subtropical high is accompanied by an eastward extension of the MT. Because of the modulation of ENSO on the WNP subtropical high (Wang et al. 2000; Wu et al. 2003), an anomalous MT may be a key actor that bridges ENSO and TC activity over the WNP.

Previous studies on the variability of TC activity have focused on investigating variations in the MT. Results show that the location of the MT exhibits a primary control on the distribution of TC activity over the WNP. Most of these studies suggested that roughly more than 70% of WNP TC geneses are linked to the MT (Briegel and Frank 1997; Chen et al. 2004; Ritchie and Holland 1999; Ritchie 1995). Note that the TD-type disturbance refers to the classical tropical wave types known to have a strong impact on tropical cyclogenesis. The displacement of the maximum genesis frequency of TCs follows that of the MT. The intraseasonal variability of the MT (Zhou and Chan 2005) may modulate TC activity (Chen et al. 2009, 2010). As observed by Sadler (1967), Frank (1987), Chia and Ropelewski (2002), and Chen et al. (1998, 2006), the MT is a favorable region for TC genesis because it provides an environment of large low-level cyclonic vorticity. Harr and Elsberry (1991, 1995) demonstrated that variability in low-level zonal wind anomalies, which signify the strength of the MT over the WNP, have a significant impact on the location and track of TCs.

The linkage between the WNP TC activity and the MT, however, is not fully understood. To date, changes in the number, genesis location, lifetime, track, and intensity of TCs during the years when the MT is in different states have not been documented. Here, we focus on investigations of all these characteristics of TC variability over the WNP and their linkage with the variability of the MT.

In this study, we consider that the TC activity is affected by the MT in the following two important ways. One is the large-scale environmental condition that may trigger TC formation and favor TC development. The monsoon circulations near the MT are closely related to several primary environmental factors defined initially by Gray (1968, 1975) to be favorable for TC genesis (Harr and Chan 2005). Another important way for TC formation is the prior existence of enhanced low-level synoptic-scale disturbances (Zehr 1992; Sobel and Maloney 2000), such as mixed Rossby-gravity (MRG) waves and (tropical depression) TD-type disturbances in the WNP (e.g., Frank and Roundy 2006; Zhou and Wang 2007; Chen and Huang 2009; Aiyyer and Molinari 2003; Dickinson and

Molinari 2002). The MT is a background field favorable for the growth of synoptic-scale wave disturbances. Gray (1998) found that a westward-moving cloud cluster entering a stationary MT can bring about an effective wind surge on the equatorward side of the trough and convection becomes rapidly enhanced. Shapiro (1977) and Zehnder (1991) proposed that synoptic-scale disturbances act as a possible forcing mechanism for tropical cyclogenesis through a local increase in low-level convergence and relative vorticity.

The present study investigates the relationship between the MT and TC activity, and provides an understanding of the development of low-level synoptic-scale disturbances within the MT from an energetic point of view. The article is arranged into six sections. Section 2 describes data and the data processing methods. In section 3, we present the dominant zonal fluctuations of the MT on interannual time scales. Section 4 examines the relationship between the MT and WNP TC activity on interannual time scales. The impact of the MT on TC activity over the WNP is then elucidated from large-scale circulation changes in section 5 and synoptic-scale disturbance activities are discussed in section 6. A summary of results is presented in section 7.

## 2. Data and methods

### a. Data

The best-track dataset from the Joint Typhoon Warning Center (JTWC) for the period 1979–2007 is used to construct the accumulated cyclone energy (ACE; Bell et al. 2000) and other indices of TC activity. The JTWC data contain the 6-hourly (0000, 0600, 1200, and 1800 UTC) center locations (latitude and longitude), and intensities (maximum 1-min mean sustained surface wind speeds) of TCs.

The present study uses monthly mean sea surface temperatures (SSTs) from the National Oceanic and Atmospheric Administration (NOAA) Extended Reconstructed Sea Surface Temperature (ERSST) V3b (Smith et al. 2008; Xue et al. 2003), outgoing longwave radiation (OLR) from NOAA polar-orbiting satellites (Liebmann and Smith 1996), and several daily meteorological variables from the National Centers for Environmental Prediction (NCEP) Department of Energy (DOE) reanalysis version 2 (hereafter as NCEP2; Kanamitsu et al. 2002) during the period 1979–2007. Only the data from July to November, which is the so-called TC season in the WNP, are used in this study.

### b. Methods

An empirical orthogonal function (EOF) analysis (Lorenz 1956) is employed to extract dominant interannual

variations of the MT. The obtained EOF modes could provide physical insight into the principal characteristics of MT variability over the WNP. To examine and illustrate the influence of the MT on WNP TC activity, a composite analysis based on the leading EOF time coefficients is performed in this study. The statistical significance of the anomalies is estimated by the Student's *t* test. In addition, Butterworth filtering is used to isolate the signal of the synoptic-scale disturbances (with a 2–8-day period).

### 3. Zonal variation of the MT on interannual time scales

Lander (1994) and Chen et al. (1998) pointed out that the interannual variation of TC genesis may be affected by the longitudinal variation of the MT. Flow intensification on either side of the MT increases the low-level vorticity and enhances TC genesis (Frank 1987). To explore this possibility, we first investigate the dominant zonal variation of the MT on interannual time scales.

The MT was found to be close to the region of low-level cyclonic relative vorticity. The location of the MT could be defined as an axis of maximum relative vorticity (Lau and Lau 1992). To examine the zonal variability of intensity and spatial location of the MT, the extent of the MT was constructed by identifying the average latitude ( $5^{\circ}$ – $20^{\circ}$ N) of the 850-hPa positive relative vorticity for July–November in each year. Figure 1a illustrates the long-term (1979–2007) mean of the relative vorticity averaged during the TC season in the  $5^{\circ}$ – $20^{\circ}$ N latitudinal strip. The longitudinal extension of the MT ranges from  $120^{\circ}$ E– $180^{\circ}$ , as indicated by the local maximum positive vorticity (Fig. 1a). The interannual fluctuation is, however, large in both amplitude and zonal distribution, as shown in Fig. 1b. As the cyclonic vorticity in the MT increases (decreases), the easternmost location of the MT in the TC season tends to extend (retreat) eastward (westward).

To extract the dominant interannual variations that are indicated in Fig. 1b, we applied the EOF analysis to a time–longitude dataset. Figure 2 exhibits the first EOF and the corresponding normalized time coefficients. The contribution to the total variance by the first EOF mode is 66.6%. In the spatial pattern (Fig. 2a), positive values appear in the  $135^{\circ}$ – $175^{\circ}$ E longitudinal band. The temporal variation (Fig. 2b) indicates that the years of positive (negative) values are well synchronized with the eastward extension (westward retreat) of the MT. The time coefficient of the leading mode displays year-to-year fluctuations consistent with the SST anomalies in the Niño-3.4 region (Fig. 2b). Their correlation coefficient is 0.89, which exceeds the 99% confidence level. This indicates that the interannual variation of the MT is a response to ENSO. An El Niño event will lead to an increase in relative vorticity

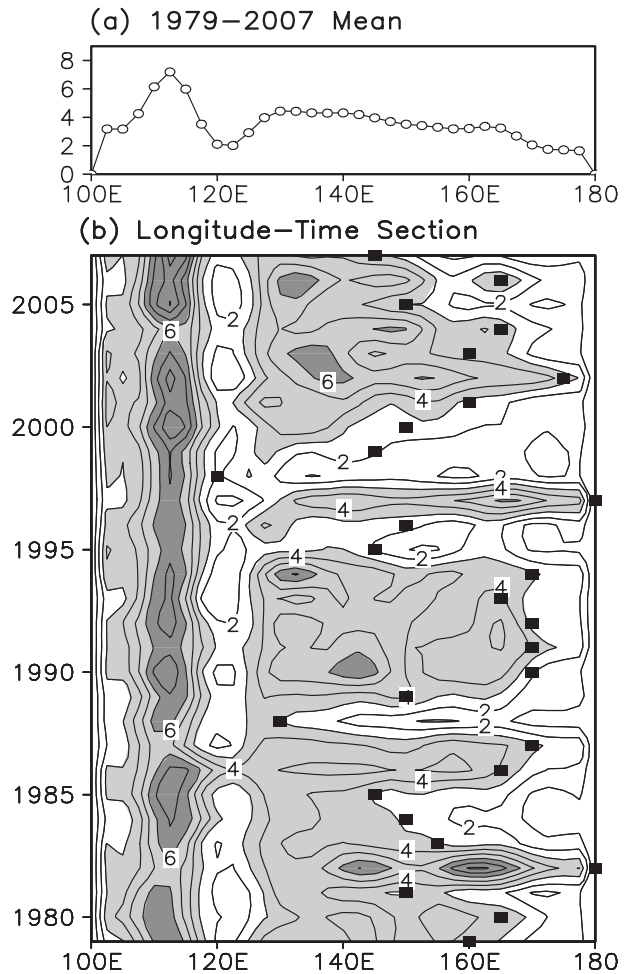


FIG. 1. July–November positive vorticity along  $5^{\circ}$ – $20^{\circ}$ N: (a) the long-term mean for the period 1979–2007 and (b) the value for individual years. The contour interval is  $1 \times 10^{-6} \text{ s}^{-1}$  in (b), and regions with values larger than  $3$  ( $6$ )  $\times 10^{-6} \text{ s}^{-1}$  are lightly (darkly) shaded. The solid squares are the farthest annual eastward extent of the MT.

over the western central tropical North Pacific and thus an eastward extension of the MT.

### 4. TC activity associated with interannual variations of the MT

Can the longitudinal variation of the MT cause the interannual variation of TC activity? To answer this question, we perform a composite analysis for anomalous MT years. Based on the time coefficients of leading EOF mode, we identify 7 yr (approximately 25% of the 29-yr period) with the highest values of the time coefficient as strong MT (S-MT) years, and the 7 yr with the lowest values of the time coefficient as weak MT (W-MT) years (see Table 1); the other 15 yr are defined as neutral MT (N-MT) years.

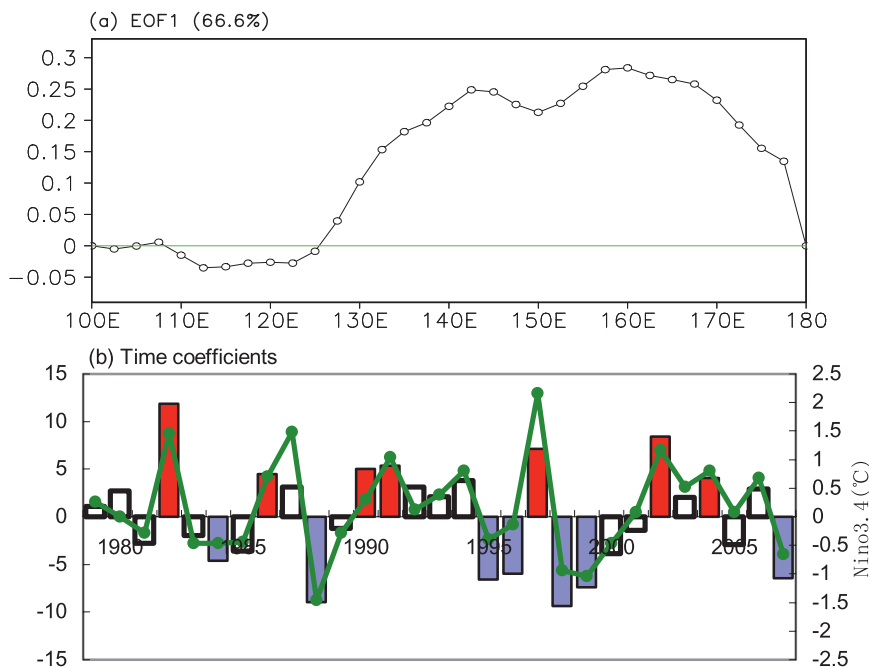


FIG. 2. (a) First EOF mode of interannual fluctuation of the July–November positive vorticity averaged over the 5°–20°N latitude strip (as in Fig. 1b) and (b) the corresponding time coefficients (bar) whose scale is shown on the left and the Niño-3.4 SST anomaly (line) with the scale on the right. The strong (weak) MT climate condition is marked by red (blue).

Figure 3 displays composite charts of the 850-hPa streamline for seven S-MT and seven W-MT years displayed in Figs. 3a and 3b, respectively. Superimposed on these two composite charts are the locations of TC genesis for corresponding years (TC seasons) and OLR. Some striking contrasts of the 850-hPa streamline and low-valued OLR between S-MT and W-MT years emerge from the comparison of Figs. 3a,b. The MT extends (retreats) eastward (westward) during S-MT (W-MT) years. The locations of the TC genesis display notable contrasts between S-MT and W-MT years as well. More TCs are generated east of 160°E in S-MT years than in W-MT years. The results indicate that the interannual variations in the location of TC genesis over the WNP are consistent with the interannual variations in the east–west extension of the MT.

To further clarify the effect of the longitudinal variation of the MT on TC genesis frequency, the mean number of TCs in four intensity ranges [tropical depression, tropical storm, typhoon (categories 1–3), and severe typhoon (categories 4–5)] for different MT years is shown in Fig. 4. There is no significant difference in the total number of TCs over the WNP. There are more (less) intense typhoons (ST, TY) in the S-MT (W-MT) years than in the N-MT years.

To obtain a sense of the spatial feature in the interannual variation of TC genesis frequencies, the aforementioned

analysis domain is divided into five subregions: region southwest (SW; 0°–15°N, 120°–150°E), region northwest (NW; 15°–30°N, 120°–150°E), region southeast (SE; 0°–15°N, 150°E–180°), region northeast (NE; 15°–30°N, 150°E–180°), and the South China Sea (SCS; 0°–25°N, 100°–120°E). This domain division is presented in Fig. 3. The mean number of TCs in S-MT and W-MT years in the above subregions is displayed in Fig. 5. The increase (decrease) of TC genesis in the S-MT (W-MT) years comes primarily from the region SE (Figs. 3 and 5a). Such characteristics are mainly seen in the intense TCs (typhoon; Fig. 5b). The TC genesis frequency in S-MT years is enhanced in region SE and suppressed in the other four regions. The variations are more significant in region SE. The frequency of formation of TCs in region SE during the S-MT years is about 3 times that during the W-MT years.

TABLE 1. Strong MT and weak MT, as defined from the zonal variation of the MT index in Fig. 2b.

Strong MT	Weak MT
1982	1984
1986	1988
1990	1995
1991	1996
1997	1998
2002	1999
2004	2007

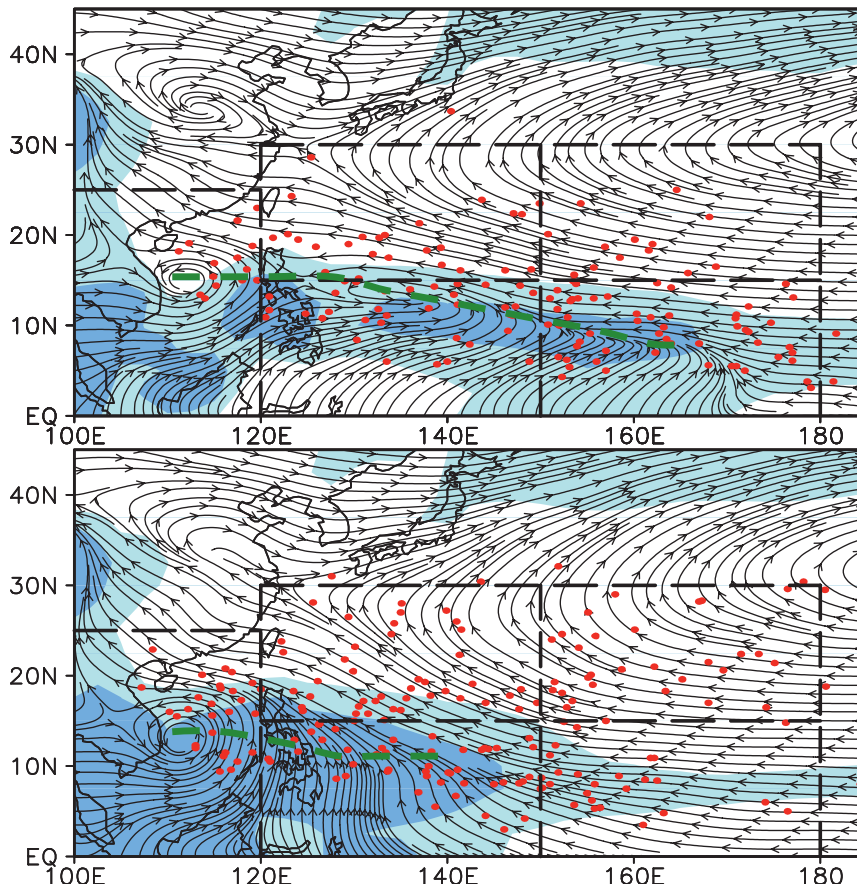


FIG. 3. The 850-hPa streamline charts with superimposed OLR for average of (top) seven S-MT years and (bottom) seven W-MT years during the TC season. The solid red dots represent the locations of TCs identified at the beginnings of their life cycles. The MT is denoted by a green, thick-dashed line. Note that areas of  $OLR < 218 \text{ W m}^{-2}$  are heavily shaded, and areas of  $218 \text{ W m}^{-2} < OLR < 230 \text{ W m}^{-2}$  are lightly shaded.

Previous works have noted that the life span, intensity, and the location of formation of TCs are intimately related (Camargo and Sobel 2005; Camargo et al. 2007; Wang and Chan 2002). Wu and Wang (2004) suggested that the shift of formation locations can have a larger influence on tracks than the projected changes in large-scale steering flows. In other words, the interannual variations of TC activity have been attributed to the shift in the location of the TC genesis. Figure 6 shows the mean lifetimes of TCs in the different TC genesis regions for S-MT, N-MT, and W-MT years. There is no significant shift toward longer or shorter lifetimes in different MT years. However, the TC has a significant shift toward a longer lifetime when it is generated in the SE sector. This tendency toward a longer lifetime could explain the well-documented effect of the location of TC genesis on the mean lifetime.

Figure 7a shows the difference between the S-MT and W-MT years in the mean frequency of TC occurrence during the TC season for each  $2.5^\circ \times 2.5^\circ$  grid. The

maximum difference in the frequency of occurrence is used to infer the difference in the prevailing tracks. During S-MT years, there is a significant increase in the northwestward tracks, which start in the SE quadrant of

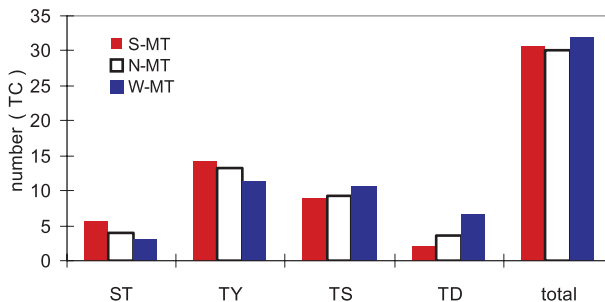


FIG. 4. Average number of TCs (1979–2007) based on the Saffir–Simpson scale and additional classifications for S-MT (red), N-MT (white), and W-MT (blue) years. Tropical depression (TD), tropical storms (TS), category-1–3 typhoons (TY), and category-4–5 typhoons (ST). Unit is  $\text{yr}^{-1}$ .

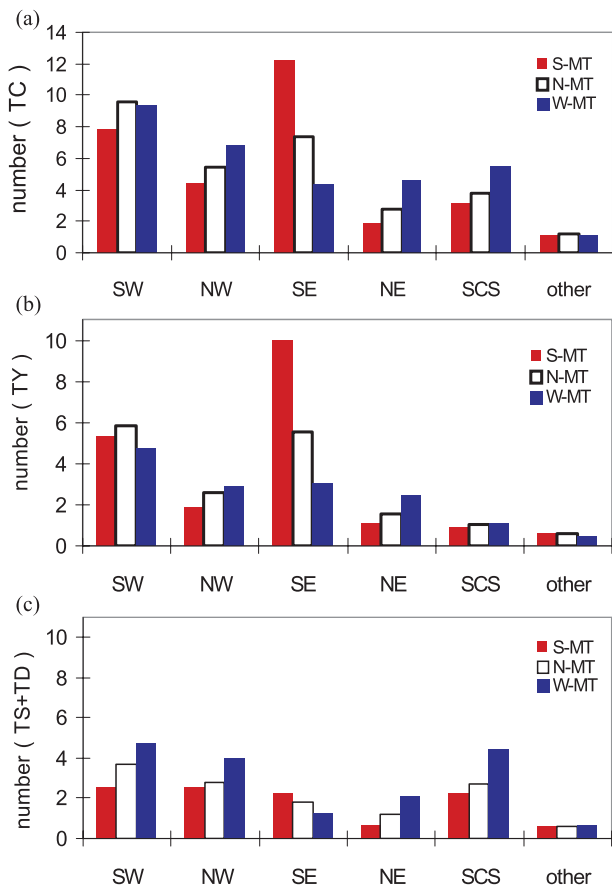


FIG. 5. Mean number of (a) TC, (b) TY, and (c) TS + TD genesis per year over each region of Fig. 3 in S-MT (red), N-MT (white), and W-MT (blue) years.

the WNP and tend to recurve from northwestward to northeastward around 25°N, 130°E. In addition, the frequency of a northwestward path toward Japan is significantly higher than that during the W-MT years.

To represent spatial distribution of TC activity, the difference in the ACE patterns in S-MT and W-MT years is shown in Fig. 7b. There is an increase in ACE values in most of the basin, with a pronounced maximum at 20°N, 140°E. The ACE distribution displays a clear east–west pattern, with more TC activity east of the Philippines than in the South China Sea. Though the sample size is small, differences between the S-MT and W-MT years are evident. The entire distribution of ACE per year in S-MT (W-MT) years is shifted to larger (smaller) values, and the differences between S-MT and W-MT years are statistically significant. This is affected by the characteristics of TC track as well as TC intensity and lifetime, related to the shift in the locations of genesis associated with the zonal migration of the MT. In other words, corresponding to more TCs in the region SE, the TC activity shifted south-eastward and the TCs are more intense during S-MT years.

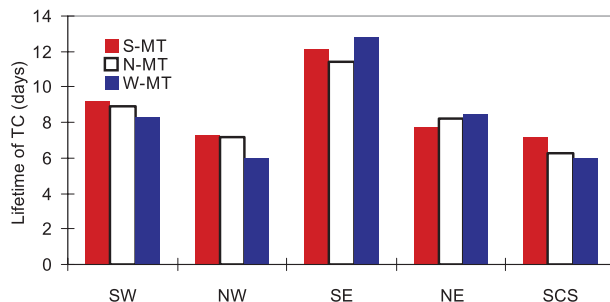


FIG. 6. As in Fig. 5a, but for TC lifetimes per year in S-MT (red), N-MT (white), and W-MT (blue) years.

The above analyses reveal obvious differences between S-MT and W-MT years in the TC intensity, track, and ACE. These differences suggest that there may be differences in the genesis locations between these two extreme MT states. Since the S-MT and W-MT years are related to changes in the large-scale circulation and synoptic-scale disturbances over the WNP, such changes should also explain these observed anomalies in TC genesis, which will be discussed in the next section.

### 5. Large-scale circulation changes

Many previous studies have demonstrated that TC formation and development are associated with the

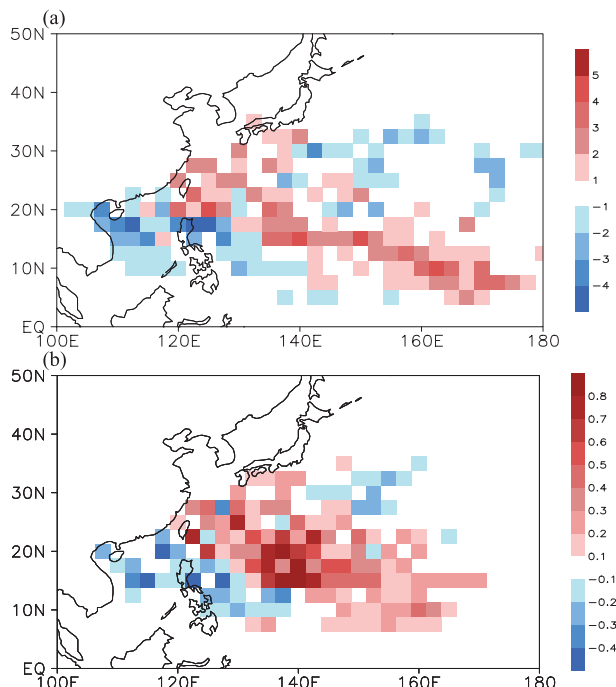


FIG. 7. Difference between anomalies in S-MT and W-MT years of the (a) total number of TC occurrences in each 2.5° × 2.5° grid and (b) ACE. Units for number of TC are yr<sup>-1</sup> and for ACE is 10<sup>5</sup> m<sup>2</sup> s<sup>-2</sup> yr<sup>-1</sup>.

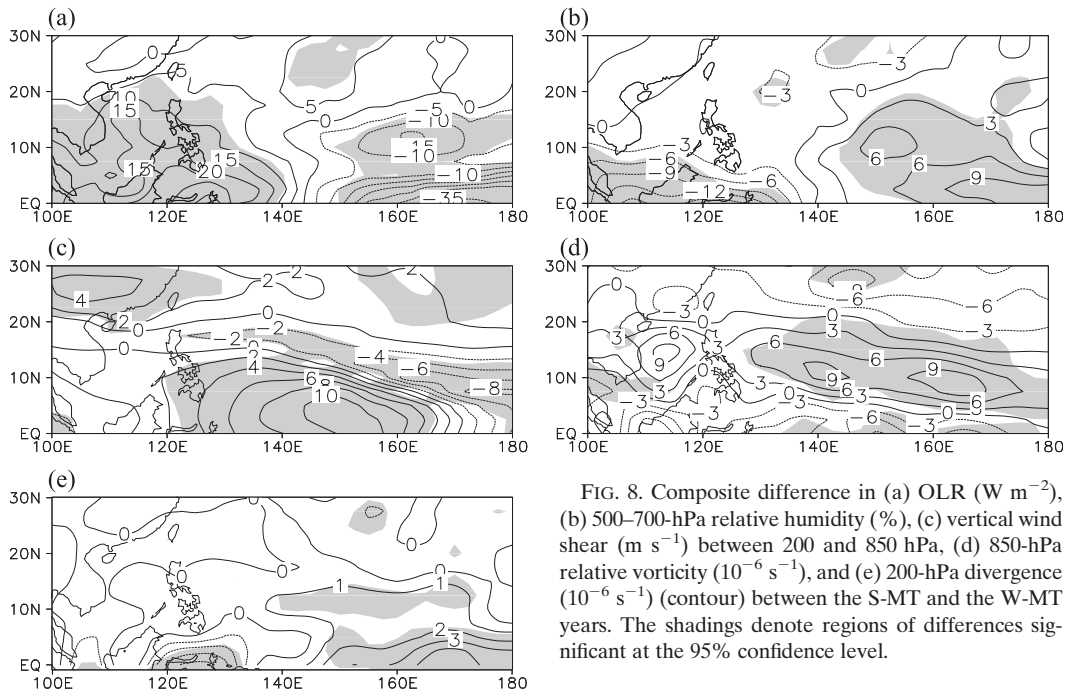


FIG. 8. Composite difference in (a) OLR ( $\text{W m}^{-2}$ ), (b) 500–700-hPa relative humidity (%), (c) vertical wind shear ( $\text{m s}^{-1}$ ) between 200 and 850 hPa, (d) 850-hPa relative vorticity ( $10^{-6} \text{ s}^{-1}$ ), and (e) 200-hPa divergence ( $10^{-6} \text{ s}^{-1}$ ) (contour) between the S-MT and the W-MT years. The shadings denote regions of differences significant at the 95% confidence level.

large-scale environmental changes. The variables examined in previous studies (e.g., Briegel and Frank 1997; Chan and Liu 2004; Cheung 2004; Chu 2002; Ramsay et al. 2008; Sobel and Camargo 2005; Wu and Chu 2007) are 1) OLR, 2) 500–700-hPa relative humidity (RH), 3) 200–850-hPa vertical wind shear, 4) upper-level divergence, and 5) low-level vorticity.

Figure 8a displays the OLR difference between the S-MT and W-MT years. It shows a somewhat east–west-oriented low-OLR region along the equator and 12°N, with significant reduced values (stronger convection) up to  $-10 \text{ W m}^{-2}$  in the SE region concurrent with the zonal migration of the MT.

A high value of RH in the lower troposphere, which is roughly represented by the 500–700-hPa layer-mean relative humidity, is favorable for TC formation (Cheung 2004). The differences in 500–700-hPa relative humidity (Fig. 8b) are similar to those in OLR, with increased values up to 6% in the SE region that is basically in the MT region.

An increase in the formation of TCs usually occurs in a low vertical wind shear environment because strong vertical wind shear disrupts the development of organized deep convection, and thus limits the chance of building up a center with an upper-level warm core and large vorticity (Cheung 2004; Chu 2002; DeMaria 1996). The 200–850-hPa vertical wind shear (VWS) is defined as follows:

$$\text{VWS} = [(u_{200\text{hPa}} - u_{850\text{hPa}})^2 + (v_{200\text{hPa}} - v_{850\text{hPa}})^2]^{1/2},$$

where  $u$  and  $v$  are the zonal and meridional wind components, respectively. The difference in vertical wind shear between the two types of years is shown in Fig. 8c. There is a statistically significant decrease of VWS in the SE region in the S-MT years. Additionally, it is interesting to note that the difference over the SE is as large as  $4 \text{ m s}^{-1}$  and the crucial vertical shear line, as represented by the  $10 \text{ m s}^{-1}$  isotach (Chu 2002), shifts eastward along the MT in the S-MT years, implying a larger tropical area of weak VWS in the S-MT years.

Strong upper-level divergence in the vicinity of a low-level cyclonic vorticity enhances the possibility of development of deep convection, and thus is often favorable for TC activity (Cheung 2004). The difference in the 850-hPa relative vorticity, which is shown in Fig. 8d, displays positive vorticity anomalies predominating around the MT locations in the S-MT years. This is because the low-level cyclonic vorticity maximum over the WNP during the TC season is usually located along the MT. A band of significant increase of low-level cyclonic vorticity approximately follows the MT and stretches from 130°E to the date line, associated with the zonal variation of the MT (Fig. 2). The distribution of the 200-hPa divergence difference shows a good agreement with the difference in the 850-hPa relative vorticity (Fig. 8e).

During the S-MT years, the well-established MT is consistent with the greater low-level cyclonic vorticity, upper-level anomalous divergence, lower OLR, higher 500–700-hPa relative humidity, and weaker vertical wind shear (Fig. 8) within the SE region. Those primary

large-scale circulation changes approximately follow the eastward expansion of the MT in the adjacent region, such that they may significantly influence regional TC formation and track.

**6. Interannual variation of synoptic-scale disturbance activity**

*a. Observed relationship*

The synoptic-scale disturbances have been presented as a possible forcing mechanism for tropical cyclogenesis (Chen and Weng 1998). Those synoptic-scale disturbances in the MT environment are often associated with westward-propagating wave disturbances in the easterlies, such as MRG waves and TD-type disturbances. The characteristics of the synoptic-scale disturbance activity can be described by the eddy kinetic energy (EKE), calculated from the eddy winds ( $u'$ ,  $v'$ ):

$$EKE = \frac{1}{2}(\overline{u'^2} + \overline{v'^2}),$$

where the overbar represents a time average during TC seasons and prime denotes a perturbation from the time mean. These perturbations are obtained by applying a bandpass filter with a 2–8-day period to the daily data.

Figure 9 shows the 850-hPa EKE averaged over the days of the TC season over the WNP in the S-MT and W-MT years and the difference between the two types of years. Maximum EKE is observed in the MT region. Following the eastward extension of the MT, maximum EKE values extended farther eastward during the S-MT years than during the W-MT years. A large area of positive and statistically significant difference in synoptic-scale disturbances covers the tropical central Pacific to WNP (centered in the extension region of the MT) during the S-MT years (Fig. 9c). As a result, the low-level synoptic-scale disturbances are more active during the S-MT years than during the W-MT years.

The above result explains why the WNP TCs are more active during the S-MT years than during the W-MT years. The existence of a larger number of synoptic-scale disturbances is an important mechanism for TC genesis. Just as the zonal extent of synoptic-scale disturbance activity expands and contracts with the MT from year to year, the zonal extent of TC genesis locations expands with the eastward extension of the MT and contracts with the westward retreat of the MT. The major increase in synoptic-scale disturbances is observed in the region of the MT extension (i.e., the SE region).

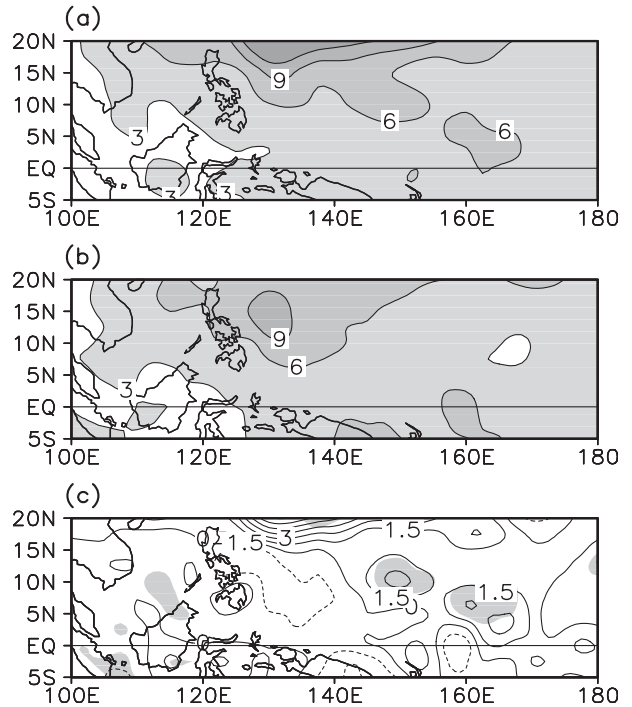


FIG. 9. Average 850-hPa EKE during the TC season (July–November) for the (a) S-MT years, (b) W-MT years, and (c) difference between (a) and (b), in units of  $m^2 s^{-2}$ . Shadings in (c) indicate areas of difference exceeding the 95% confidence level using a Student's *t* test.

*b. Physical mechanism*

The observational analysis above reveals the difference of the synoptic-scale disturbances between the S-MT and the W-MT years. To further understand how the MT-induced mean flow change modulates the activity of synoptic-scale disturbances, we diagnose the effect of the barotropic energy conversion in the growth of synoptic-scale disturbances.

For a given time-invariant basic state, the conversion from the basic state (MT) to the EKE is encapsulated in the following expression (Maloney and Hartmann 2001):

$$\begin{aligned} \frac{\partial}{\partial t} K'_{\text{baro}} = \{ \overline{K}, K' \} &= -\overline{u'v'} \frac{\partial \overline{u}}{\partial y} - \overline{u'v'} \frac{\partial \overline{v}}{\partial x} \\ &\quad - \overline{u'^2} \frac{\partial \overline{u}}{\partial x} - \overline{v'^2} \frac{\partial \overline{v}}{\partial y}, \end{aligned}$$

where the overbar represents a time average and the prime a deviation; and  $u$ ,  $v$ , and  $K$  represent zonal and meridional velocity, and the kinetic energy, respectively. We have computed the barotropic conversion term ( $\partial K'_{\text{baro}} / \partial t$ ) from the 850-hPa wind data. The overbar is not computed by an average over the whole data record, but average during the TC season. The prime is defined using 2–8-day bandpass-filtered fields.



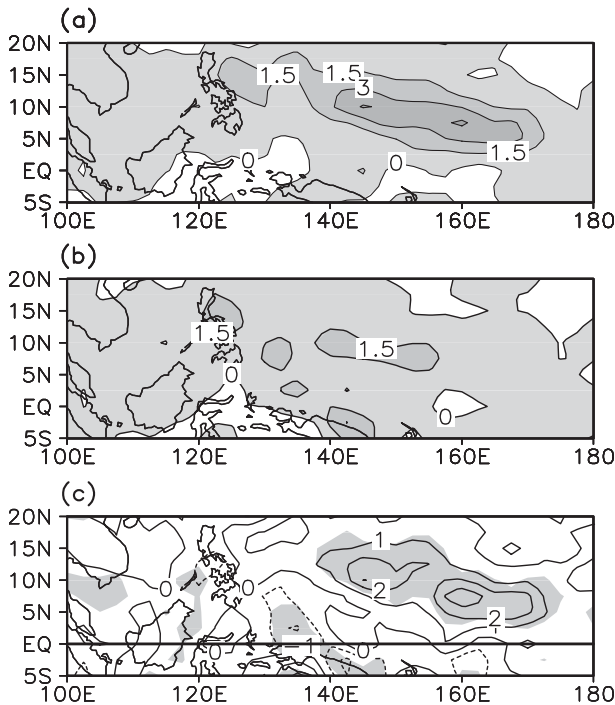


FIG. 10. The horizontal distribution of the 850-hPa EKE time change rate due to the barotropic energy conversion (unit:  $10^{-5} \text{ m}^2 \text{ s}^{-3}$ ) during the TC season (July–November) for (a) S-MT composite, (b) W-MT composite, and (c) their difference (S-MT composite minus W-MT composite). Shadings in (c) indicate areas where the difference is significant at the 95% level based on the Student's  $t$  test.

The top two panels of Fig. 10 show the composite of barotropic conversion term in the S-MT and the W-MT years, respectively. In both cases, a longitudinally oriented tongue of maxima is seen in the MT region around  $5^{\circ}$ – $20^{\circ}$ N, indicating local eddy growth through barotropic eddy–mean flow interactions. The tongue of large energy tendency also shifts remarkably eastward, concurrent with the eastward extension of the MT in the S-MT years. The bottom panel (Fig. 10c) shows the difference between the two types of years, Fig. 10a minus Fig. 10b. This plot indicates that the magnitude of the barotropic conversion term averaged over the tongue is larger in the S-MT years than in the W-MT years. The anomalous barotropic energy conversion term is significant in the SE region where the MT expands eastward (retreats westward) during the S-MT (W-MT) years. The result implies that the more (less) rapid growth of the perturbation during the S-MT (W-MT) years is attributed to more (less) efficient low-level barotropic energy conversion. Thus, the MT-induced mean flow change modulates the energy conversion between the mean flow and the synoptic eddies and determines the local growth rate of the synoptic-scale disturbances and thus the frequency of TC genesis.

We have also performed a diagnosis of wave propagation, such as the barotropic version of Plumb's (1986) wave activity flux formulation that was applied by Sobel and Bretherton (1999). Indeed, the results of wave propagation diagnosis are very similar to those of the energetic diagnosis.

## 7. Conclusions

The possible linkage between MT variability and TC activity over the WNP has been analyzed in this study. It is found that the frequency of TC formation increases remarkably in the SE region ( $0^{\circ}$ – $15^{\circ}$ N,  $150^{\circ}$ E– $180^{\circ}$ ) and decreases in the other regions during the S-MT years. When the MT extends eastward in the tropical WNP to around  $160^{\circ}$ E, TC activity is above normal over most parts of the WNP east of  $\sim 125^{\circ}$ E, and slightly fewer TCs tend to occur near the Philippines and the South China Sea (SCS). The present study also shows that there is a tendency in the S-MT years toward both more intense and longer-lived TCs than in the W-MT years.

Previous studies have shown the modulation of ENSO on the TC activity over the WNP (Chan 1985, 2000; Sobel and Camargo 2005; Camargo et al. 2007; Chia and Ropelewski 2002; Wang and Chan 2002; Zhan et al. 2011; Chen and Weng 1998). In the El Niño years, the TC genesis position shifts southeastward and TCs have longer lifetimes and are stronger. This ENSO–TC relationship is likely to be explained by changes in the large-scale circulation associated with the MT. In view of the link between ENSO and the MT, the MT acts as a medium connecting the ENSO to the TC activity over the WNP. It should be noted that other factors could also affect the TC activity over the WNP through modulating the MT, such as the Indian Ocean SST (Zhan et al. 2011; Zhou et al. 2005) and the Hadley circulation signal (Zhou and Cui 2008), but these are not examined here.

The modulation of the MT on the TC genesis has been shown in many previous studies from a synoptic perspective (e.g., Harr and Elsberry 1995; Ritchie and Holland 1999; Chen et al. 2009, 2010). The present study shows the influence of the MT on the interannual variation of the TC genesis over the SE region where the interannual variations of WNP TC genesis are most pronounced. A strong MT is followed by enhanced convection, increased relative humidity in the lower and midtroposphere, reduced vertical zonal wind shear, stronger upper-level divergence, and low-level vorticity over the region SE, which are favorable factors for TC genesis, while a weak MT is not. The synoptic-scale disturbance activity may offer a physical explanation of why more frequent TCs form in the southeast region of the WNP during the S-MT years. The eastward-extending MT during the S-MT

years may interact with the synoptic-scale disturbances and lead to the growth of perturbations as the MT is maintained in the WNP around 160°E. The MT favors the growth of the perturbations through the barotropic energy conversion and results in more tropical cyclogenesis in the southeast quadrant of the WNP.

*Acknowledgments.* This work was supported by the National Natural Science Foundation of China-Regional Cooperation Project under Grant 40921160379, the National Basic Research Program of China under Grant 2009CB421404, the National Nature Science Foundation of China under Grant 40730951, the Special Scientific Research Project for Public Interest under Grant GYNY201006021, and the Chinese Academy of Sciences under Grant KZCX2-EW-QN204.

## REFERENCES

- Aiyyer, A. R., and J. Molinari, 2003: Evolution of mixed Rossby-gravity waves in idealized MJO environments. *J. Atmos. Sci.*, **60**, 2837–2855.
- Bell, G. D., and Coauthors, 2000: Climate assessment for 1999. *Bull. Amer. Meteor. Soc.*, **81**, S1–S50.
- Briegel, L. M., 2002: *The Structure and Variability of the ITCZ of the Western North Pacific*. The Pennsylvania State University, 198 pp.
- , and W. M. Frank, 1997: Large-scale influences on tropical cyclogenesis in the western North Pacific. *Mon. Wea. Rev.*, **125**, 1397–1413.
- Camargo, S. J., and A. H. Sobel, 2005: Western North Pacific tropical cyclone intensity and ENSO. *J. Climate*, **18**, 2996–3006.
- , K. A. Emanuel, and A. H. Sobel, 2007: Use of a genesis potential index to diagnose ENSO effects on tropical cyclone genesis. *J. Climate*, **20**, 4819–4834.
- Chan, J. C. L., 1985: Tropical cyclone activity in the northwest Pacific in relation to the El Niño/Southern Oscillation phenomenon. *Mon. Wea. Rev.*, **113**, 599–606.
- , 2000: Tropical cyclone activity over the western North Pacific associated with El Niño and La Niña events. *J. Climate*, **13**, 2960–2972.
- , and K. S. Liu, 2004: Global warming and western North Pacific typhoon activity from an observational perspective. *J. Climate*, **17**, 4590–4602.
- Chan, S., and J. Evans, 2002: Comparison of the structure of the ITCZ in the west Pacific during the boreal summers of 1989–93 using AMIP simulations and ECMWF reanalyses. *J. Climate*, **15**, 3549–3568.
- Chen, G., and R. Huang, 2009: Interannual variations in mixed Rossby-gravity waves and their impacts on tropical cyclogenesis over the western North Pacific. *J. Climate*, **22**, 535–549.
- Chen, T.-C., and S.-P. Weng, 1998: Interannual variation of the summer synoptic-scale disturbance activity in the western tropical Pacific. *Mon. Wea. Rev.*, **126**, 1725–1733.
- , —, N. Yamazaki, and S. Kiehne, 1998: Interannual variation in the tropical cyclone formation over the western North Pacific. *Mon. Wea. Rev.*, **126**, 1080–1090.
- , S.-Y. Wang, M.-C. Yen, and W. A. Gallus Jr., 2004: Role of the monsoon gyre in the interannual variation of tropical cyclone formation over the western North Pacific. *Wea. Forecasting*, **19**, 776–785.
- , —, and —, 2006: Interannual variation of the tropical cyclone activity over the western North Pacific. *J. Climate*, **19**, 5709–5720.
- , —, —, and A. J. Clark, 2009: Impact of the intraseasonal variability of the western North Pacific large-scale circulation on tropical cyclone tracks. *Wea. Forecasting*, **24**, 646–666.
- , J.-D. Tsay, M.-C. Yen, and E. O. Cayan, 2010: Formation of the Philippine twin tropical cyclones during the 2008 summer monsoon onset. *Wea. Forecasting*, **25**, 1317–1341.
- Cheung, K. K. W., 2004: Large-scale environmental parameters associated with tropical cyclone formations in the western North Pacific. *J. Climate*, **17**, 466–484.
- Chia, H.-H., and C. F. Ropelewski, 2002: The interannual variability in the genesis location of tropical cyclones in the northwestern Pacific. *J. Climate*, **15**, 2934–2944.
- Chu, P.-S., 2002: Large-scale circulation features associated with decadal variations of tropical cyclone activity over the central North Pacific. *J. Climate*, **15**, 2678–2688.
- DeMaria, M., 1996: The effect of vertical shear on tropical cyclone intensity change. *J. Atmos. Sci.*, **53**, 2076–2087.
- Dickinson, M., and J. Molinari, 2002: Mixed Rossby-gravity waves and western Pacific tropical cyclogenesis. Part I: Synoptic evolution. *J. Atmos. Sci.*, **59**, 2183–2196.
- Frank, W. M., 1987: Tropical cyclone formation. *A Global View of Tropical Cyclones*, R. L. Elsberry, Ed., Office of Naval Research, 53–90.
- , and P. E. Roundy, 2006: The role of tropical waves in tropical cyclogenesis. *Mon. Wea. Rev.*, **134**, 2397–2417.
- Gray, W. M., 1968: Global view of the origin of tropical disturbances and storms. *Mon. Wea. Rev.*, **96**, 669–700.
- , 1975: Tropical cyclone genesis. Dept. of Atmospheric Science Paper 234, Colorado State University, Ft. Collins, CO, 121 pp.
- , 1998: The formation of tropical cyclones. *Meteor. Atmos. Phys.*, **67**, 37–69.
- Harr, P. A., and R. L. Elsberry, 1991: Tropical cyclone track characteristics as a function of large-scale circulation anomalies. *Mon. Wea. Rev.*, **119**, 1448–1468.
- , and —, 1995: Large-scale circulation variability over the tropical western North Pacific. Part I: Spatial patterns and tropical cyclone characteristics. *Mon. Wea. Rev.*, **123**, 1225–1246.
- , and J. C. L. Chan, 2005: Monsoon impacts on tropical cyclone variability. *The Global Monsoon System: Research and Forecast*, C.-P. Chang, B. Wang, and N.-C. G. Lau, Eds., Secretariat of the World Meteorological Organization, 512–542.
- Holland, G. J., 1995: Scale interaction in the western Pacific monsoon. *Meteor. Atmos. Phys.*, **56**, 57–79.
- Kanamitsu, M., W. Ebisuzaki, J. Woollen, S.-K. Yang, J. J. Hnilo, M. Fiorino, and G. L. Potter, 2002: NCEP-DOE AMIP-II Reanalysis (R-2). *Bull. Amer. Meteor. Soc.*, **83**, 1631–1643.
- Lander, M. A., 1994: An exploratory analysis of the relationship between tropical storm formation in the western North Pacific and ENSO. *Mon. Wea. Rev.*, **122**, 636–651.
- , 1996: Specific tropical cyclone track types and unusual tropical cyclone motions associated with a reverse-oriented monsoon trough in the western North Pacific. *Wea. Forecasting*, **11**, 170–186.
- Landsea, C. W., 2000: El Niño–Southern Oscillation and the seasonal predictability of tropical cyclones. *El Niño: Impacts of Multiscale Variability on Natural Ecosystems and Society*, H. F. Diaz and V. Markgraf, Eds., Cambridge University Press, 149–181.

- Lau, K.-H., and N.-C. Lau, 1992: The energetics and propagation dynamics of tropical summertime synoptic-scale disturbances. *Mon. Wea. Rev.*, **120**, 2523–2539.
- Lau, K.-M., and M. T. Li, 1984: The monsoon of East Asia and its global associations—A survey. *Bull. Amer. Meteor. Soc.*, **65**, 114–125.
- Liebmann, B., and C. A. Smith, 1996: Description of a complete (interpolated) OLR dataset. *Bull. Amer. Meteor. Soc.*, **77**, 1275–1277.
- Lorenz, E. N., 1956: Empirical orthogonal functions and statistical weather prediction. Scientific Rep. 1, Statistical Forecasting Project, MIT, Cambridge, MA, 48 pp.
- Maloney, E. D., and D. L. Hartmann, 2001: The Madden-Julian oscillation, barotropic dynamics, and North Pacific tropical cyclone formation. Part I: Observations. *J. Atmos. Sci.*, **58**, 2545–2558.
- Plumb, R. A., 1986: Three-dimensional propagation of transient quasigeostrophic eddies and its relationship with the eddy forcing of the time-mean flow. *J. Atmos. Sci.*, **43**, 1657–1678.
- Ramsay, H. A., L. M. Leslie, P. J. Lamb, M. B. Richman, and M. Leplastrier, 2008: Interannual variability of tropical cyclones in the Australian region: Role of large-scale environment. *J. Climate*, **21**, 1083–1103.
- Ritchie, E. A., 1995: Mesoscale aspects of tropical cyclone formation. Ph.D. dissertation, Monash University, 167 pp. [Available from Monash University, Wellington Rd., Clayton, VIC 3168, Australia.]
- , and G. J. Holland, 1999: Large-scale patterns associated with tropical cyclogenesis in the western Pacific. *Mon. Wea. Rev.*, **127**, 2027–2043.
- Sadler, J. C., 1967: On the origin of tropical vortex. *Proc. Working Panel on Tropical Dynamic Meteorology*, Norfolk, VA, Naval Weather Research Facility, 39–75.
- Shapiro, L. J., 1977: Tropical storm formation from easterly waves: A criterion for development. *J. Atmos. Sci.*, **34**, 1007–1022.
- Smith, T. M., R. W. Reynolds, T. C. Peterson, and J. Lawrimore, 2008: Improvements to NOAA's historical merged land-ocean surface temperature analysis (1880–2006). *J. Climate*, **21**, 2283–2296.
- Sobel, A. H., and C. S. Bretherton, 1999: Development of synoptic-scale disturbances over the summertime tropical northwest Pacific. *J. Atmos. Sci.*, **56**, 3106–3127.
- , and E. D. Maloney, 2000: Effect of ENSO and the MJO on western North Pacific tropical cyclones. *Geophys. Res. Lett.*, **27**, 1739–1742.
- , and S. J. Camargo, 2005: Influence of western North Pacific tropical cyclones on their large-scale environment. *J. Atmos. Sci.*, **62**, 3396–3407.
- Tomita, T., T. Yoshikane, and T. Yasunari, 2004: Biennial and lower-frequency variability observed in the early summer climate in the western North Pacific. *J. Climate*, **17**, 4254–4266.
- Wang, B., and R. Wu, 1997: Peculiar temporal structure of the South China Sea summer monsoon. *Adv. Atmos. Sci.*, **14**, 177–194.
- , and J. C. L. Chan, 2002: How strong ENSO events affect tropical storm activity over the western North Pacific. *J. Climate*, **15**, 1643–1658.
- , R. Wu, and X. Fu, 2000: Pacific–East Asian teleconnection: How does ENSO affect East Asian climate? *J. Climate*, **13**, 1517–1536.
- Webster, P. J., 1980: A model of the seasonally varying planetary scale monsoon. *Monsoon Dynamics*, J. Lighthill and R. P. Pearce, Eds., Cambridge University Press, 165–192.
- Wu, L., and B. Wang, 2004: Assessing impacts of global warming on tropical cyclone tracks. *J. Climate*, **17**, 1686–1698.
- Wu, P., and P.-S. Chu, 2007: Characteristics of tropical cyclone activity over the eastern North Pacific: The extremely active 1992 and the inactive 1977. *Tellus*, **59A**, 444–454.
- Wu, R., Z.-Z. Hu, and B. P. Kirtman, 2003: Evolution of ENSO-related rainfall anomalies in East Asia. *J. Climate*, **16**, 3741–3757.
- Xue, Y., T. M. Smith, and R. W. Reynolds, 2003: Interdecadal changes of 30-yr SST normals during 1871–2000. *J. Climate*, **16**, 1601–1612.
- Zehnder, J. A., 1991: The interaction of planetary-scale tropical easterly waves with topography: A mechanism for the initiation of tropical cyclones. *J. Atmos. Sci.*, **48**, 1217–1230.
- Zehr, R. M., 1992: Tropical cyclogenesis in the western North Pacific. U.S. Dept. of Commerce, 181 pp.
- Zhan, R., Y. Wang, and X. Lei, 2011: Contributions of ENSO and east Indian Ocean SSTA to the interannual variability of northwest Pacific tropical cyclone frequency. *J. Climate*, **24**, 509–521.
- Zhou, B., and X. Cui, 2008: Hadley circulation signal in the tropical cyclone frequency over the western North Pacific. *J. Geophys. Res.*, **113**, D16107, doi:10.1029/2007JD009156.
- Zhou, W., and J. C. L. Chan, 2005: Intraseasonal oscillations and the South China Sea summer monsoon onset. *Int. J. Climatol.*, **25**, 1585–1609.
- , —, and C. Y. Li, 2005: South China Sea summer monsoon onset in relation to the off-equatorial ITCZ. *Adv. Atmos. Sci.*, **22**, 665–676.
- Zhou, X., and B. Wang, 2007: Transition from an eastern Pacific upper-level mixed Rossby-gravity wave to a western Pacific tropical cyclone. *Geophys. Res. Lett.*, **34**, L24801, doi:10.1029/2007GL031831.